

# Determining wave propagation characteristics of MV XLPE power cable using time domain reflectometry technique

Ghulam Murtaza HASHMI<sup>1</sup>, Ruslan PAPAZYAN<sup>2</sup>, Matti LEHTONEN<sup>3</sup>

<sup>1</sup>Power Systems and High Voltage Engineering, Helsinki University of Technology, (TKK), 02015, Espoo-FINLAND  
e-mail: murtaza.hashmi@tkk.fi

<sup>2</sup>Department of Electrical Systems, KTH Royal Institute of Technology, SE-100 44, Stockholm-SWEDEN  
e-mail: ruslan@kth.se

<sup>3</sup>Power Systems and High Voltage Engineering, Helsinki University of Technology, (TKK), 02015, Espoo-FINLAND  
e-mail: matti.lehtonen@tkk.fi

## Abstract

*In this paper, the wave propagation characteristics of single-phase medium voltage (MV) cross-linked polyethylene (XLPE) power cable are determined using time domain reflectometry (TDR) measurement technique. TDR delivers the complex propagation constant (attenuation and phase constant) of lossy cable transmission line as a function of frequency. The frequency-dependent propagation velocity is also determined from the TDR measurements through the parameters extraction procedure. The calibration of the measuring system (MS) is carried-out to avoid the effect of multiple reflections on the accuracy of measurements. The results obtained from the measurements can be used to localize the discontinuities as well as the design of communication through distribution power cables.*

**Key Words:** *Cross-linked polyethylene, distribution power cables, time domain reflectometry, propagation constant, attenuation constant, phase constant, propagation velocity.*

## 1. Introduction

The use of solid dielectric power cables for underground transmission/distribution has been increasing over the past twenty years. This trend is likely to continue, with steady improvement in cable material, insulation, and manufacturing process. While the primary purpose of these transmission/distribution lines is to deliver power at 50 or 60 Hz, they are also capable of carrying high frequency signals reasonably well; i.e., their high frequency performance is comparable to some commercial RF coaxial cables. Consequently, this capability is likely to be utilized more and more in the future for applications such as diagnostics, system protection, and load management. While there is some data available on the wave propagation characteristics in these conductors, there has been limited number of systematic study to date [1, 2].

The use of cross-linked polyethylene (XLPE) cables in medium voltage (MV) networks has been increasing rapidly since long. The basic material used for XLPE cable is polyethylene (PE). PE has very good electrical properties, however, its mechanical strength decreases significantly above 75 °C, thus restricting its continuous operating temperature to a certain limit. The improved thermal characteristics of PE are obtained by establishing a large number of cross-links by employing suitable techniques resulting in higher continuous current carrying capacity and short circuit temperature (250 °C) than that of PE. These cables have low dielectric losses, low environmental requirements, are light in weight, and are trouble-free in maintenance.

There is a growing interest in the study of high frequency properties of distribution lines. One major reason is the potential to use widely distributed cable networks for high capacity data communications [3]. The measurements of such studies are generally carried out at high frequencies, up to about 100 MHz, by sending pulses or signals from a point, which then travel through the conductor that essentially acts as a transmission medium. The incident and the reflected signals are analyzed. These signals are distorted or changed in one way or the other by the transmission medium, and the reconstruction techniques are applied to get the desired wave propagation characteristics (propagation constant; attenuation and phase constant, and propagation velocity) from the measurements. Frequency and time domain techniques are used, hence, the need for understanding basic electromagnetic theories and their practical applications is prerequisite [4-6].

Any signal will lose some of its energy or signal strength as it propagates down the conductor. This loss is attenuation, which is frequency-dependent. Propagation velocity is a specification of the conductor indicating the speed at which a signal travels down through it. Different conductors have different propagation velocities. Typically, propagation velocity of a communication cable under test is listed in the cable manufacturer's catalogue. However, this figure for MV power cables is not specified. In this case, a required procedure is to make TDR measurement on a known length of the conductor. A more accurate way to estimate propagation velocity is to conduct measurements from both ends of the conductor. Propagation velocity depends upon the phase constant and the frequency of the impressed signal.

Remainder of this paper is organized as follows. Section 2 presents transmission line analysis and Section 3 gives a general theoretical background of TDR. Techniques of TDR measurement is described in Section 4. Section 5 describes the procedure for parameters extraction from the measurements; and Section 6 explains calibration method for the measuring system (MS). Section 7 gives the details of TDR measurements and the wave propagation characteristics results. Section 8 presents a discussion, followed by concluding remarks given in Section 9.

## 2. Transmission line analysis

In the following analysis, the power cable is considered as a transmission channel represented by a coaxial transmission line and is approximated as a close form of the two-wire transmission line. According to [7], the two-wire transmission line must be a pair of parallel conducting wires separated by a uniform distance. Based on the above considerations, the single-phase power cable is regarded as a distributed parameter network, where voltages and currents can vary in magnitude and phase over its length. Therefore, it can be described by circuit parameters that are distributed over its length.

A differential length  $\Delta z$  of a transmission line is described by its distributed parameters  $R, L, C$ , and  $G$  as shown in Figure 1.  $R$  defines the resistance per unit length for both conductors (in  $\Omega/m$ ),  $L$  defines the inductance per unit length for the both conductors (in H/m),  $G$  is the conductance per unit length (in S/m),

and  $C$  is the capacitance per unit length (in F/m). Quantities  $v(z, t)$  and  $v(z + \Delta z, t)$  denote the instantaneous voltages at locations  $z$  and  $z + \Delta z$ , respectively. Similarly,  $i(z, t)$  and  $i(z + \Delta z, t)$  denote the instantaneous currents at the respective locations. In the circuit of Figure 1(b), applying Kirchoff's voltage and current laws, respectively, the following two equations can be obtained as [8]:

$$v(z, t) - R\Delta z \cdot i(z, t) - L\Delta z \cdot \frac{\partial i(z, t)}{\partial t} - v(z + \Delta z, t) = 0 \quad (1)$$

$$i(z, t) - G\Delta z \cdot v(z + \Delta z, t) - C\Delta z \cdot \frac{\partial v(z + \Delta z, t)}{\partial t} - i(z + \Delta z, t) = 0. \quad (2)$$

If  $v$  and  $i$  are expressed in phasor form, i.e.  $v(z, t) = \text{Re}[V(z) \cdot e^{j\omega t}]$  and  $i(z, t) = \text{Re}[I(z) \cdot e^{j\omega t}]$ , and when  $\Delta z \rightarrow 0$ , the time harmonic line equations can be derived from (1) and (2) as

$$-\frac{dV(z)}{dz} = (R + j\omega L)I(z) \quad (3)$$

$$-\frac{dI(z)}{dz} = (G + j\omega C)V(z). \quad (4)$$

The coupled time harmonic transmission line equations can be combined to solve for  $V(z)$  and  $I(z)$  as

$$\frac{d^2V(z)}{dz^2} = \gamma^2V(z) \quad (5)$$

$$\frac{d^2I(z)}{dz^2} = \gamma^2I(z), \quad (6)$$

where

$$\gamma(\omega) = \alpha(\omega) + j\beta(\omega) = \sqrt{(R + j\omega L) \cdot (G + j\omega C)}. \quad (7)$$

Here,  $\gamma$  is the propagation constant whose real and imaginary parts,  $\alpha$  and  $\beta$  are the attenuation constant (Np/m) and phase constant (rad/m) of the line respectively.  $\omega$  is the angular velocity (rad/sec), where  $\omega = 2\pi f$ , and  $f$  is the frequency (Hz) of the propagated signal. The complex propagation constant is also given as

$$\gamma(\omega) = \sqrt{Z \cdot Y}, \quad (8)$$

where  $Z = R + j\omega L$  is the series impedance per unit length and  $Y = G + j\omega C$  is the shunt admittance per unit length of the line. The characteristic impedance of the line is given as

$$Z_0 = \sqrt{\frac{R + j\omega L}{G + j\omega C}} = \sqrt{\frac{Z}{Y}}. \quad (9)$$

It is clear from (7) and (9) that  $\gamma$  and  $Z_0$  are the characteristic properties of a line whether or not the line is infinitely long. They depend on  $R$ ,  $L$ ,  $G$ ,  $C$ , and  $\omega$  but not on the line length [8].

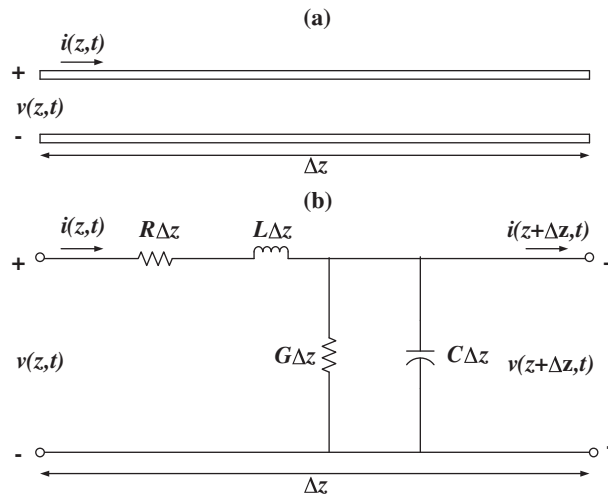


**Figure 1.** (a) The voltage and current definitions of two-wire transmission line. (b) The equivalent lumped-element circuit.

### 3. Theoretical background of TDR

The most common method for evaluating a transmission line and its load has traditionally involved applying a sine wave to a system and measuring reflected waves resulting from discontinuities on the line. From the measurements, the standing wave ratio (SWR) is calculated and used as a figure of merit for the transmission system. SWR measurements, however, fail to locate the presence of several discontinuities. In addition, when the broadband quality of a transmission system is to be determined, SWR measurements must be made at many frequencies. This method soon becomes very time consuming and tedious.

Compared to other measurement techniques, time domain reflectometry (TDR) provides a more intuitive and direct look at the characteristics of the device under test (DUT). Using a high speed oscilloscope and a pulse generator, a fast edge is launched into the transmission line under investigation. The incident and the reflected voltage waves are monitored by the oscilloscope at a particular point on the line. The block diagram of a time domain reflectometer is shown in Figure 2 [9, 10].

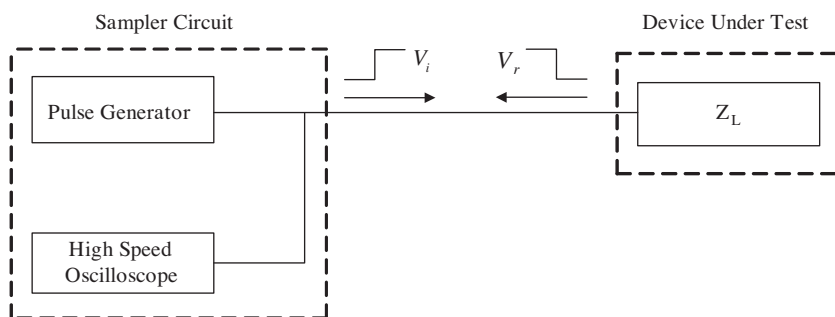


**Figure 2.** Functional block diagram of a time domain reflectometer.

Another aspect of TDR measurements is that it demonstrates whether losses in a transmission system are series or shunt losses. All of the information is immediately available from the oscilloscope's display.

Additionally, TDR gives more meaningful information concerning the broadband response of a transmission system than any other measuring technique [9].

TDR instruments work on the same principle as radar, but instead of air, they work through, in this case, wires. A pulse of energy is transmitted down a line. When the launched propagating wave reaches at the end of the line or any impedance change along the transmission line, part or all of the pulse energy is reflected back to the instrument. This reflected wave is energy that is not delivered to the load. The magnitude of the impedance change can be calculated using the reflection coefficient  $\Gamma$ , defined in the frequency domain as the ratio between the reflected voltage wave  $V_r$  and the incident voltage wave  $V_i$ . The distance to the impedance change can also be estimated knowing the speed of the propagated wave.  $\Gamma$  is related to the load impedance  $Z_L$  and the characteristic impedance of the line  $Z_0$ , by the following expression [7]

$$\Gamma = \frac{V_r}{V_i} = \frac{Z_L - Z_0}{Z_L + Z_0}. \quad (10)$$

The transmission coefficient  $T$  is given as

$$T = 1 + \Gamma = \frac{2 \cdot Z_L}{Z_L + Z_0}. \quad (11)$$

#### 4. TDR measurement setup

TDR measurements require a special test arrangement including a high speed digitizing signal analyzer (DSA) and a fast leading-edge pulse generator e.g. producing a pulse of 5 V amplitude with 10 ns pulse-width having rise-time of 200 ps. DUT is a single-phase, 95 mm<sup>2</sup> aluminum conductor, 20 kV XLPE insulated power cable having 6 m length. Although not mentioned when theoretically introducing the concept of time domain reflectrometers, there are two more components in the measurement set-up, which are of extreme importance for the quality of TDR testing. These are the T-connection needed for monitoring the incident and reflected pulses by DSA, and the connection between the measuring equipment and the DUT. Tektronix DSA 602 consists of powerful internal digital signal processors that can process digitized signals up to 180 times per second. Features include sampling rate of 2 G samples/s, 8-bit vertical resolution, and 1 GHz system bandwidth. The TDR measuring set-up including DUT and MS is arranged in an ordinary room and is depicted in Figure 3.

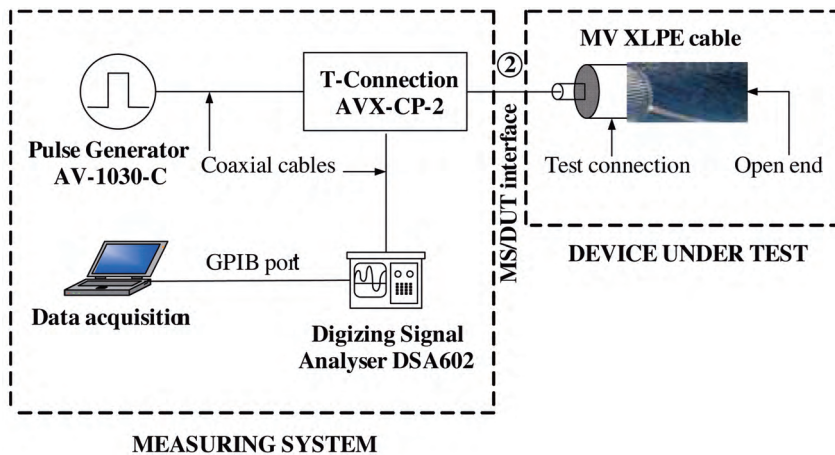


Figure 3. Schematic drawing of the TDR measuring set-up.

In practice, a narrow electric pulse is applied to the DUT and the incident and reflected waves are measured by means of a DSA at a T-connection. The measured data is transferred to the computing system (laptop) connected to the DSA through the general purpose interface bus (GPIB), where the analysis is done using MATLAB [10], [11].

## 5. TDR parameters extraction method

The propagation constant of a wave traveling along a transmission line segment of a length  $l$  is the complex voltage ratio between the output (reflected pulse  $V_{out}$ ) and the input (incident pulse  $V_{in}$ ) of the line segment [12].

If the cable is considered as a linear system, this ratio represents the cable transfer function  $H(\omega)$  and the following relation holds:

$$H(\omega) = \frac{V_{out}}{V_{in}} = e^{-\gamma(\omega)l}. \quad (12)$$

In the measuring system, the incident and the reflected pulses are measured in the time domain. For a TDR measurement,  $V_{out}$  is the signal coming back after reflection at the open end of the cable. Since the measurements are done at the input side of DUT (see Figure 3), the total traveling distance is twice the length of the DUT, i.e.  $2l$ . These time domain measurements are then transformed into the frequency domain by the use of the fast Fourier transforms (FFTs) in MATLAB.

The attenuation and phase constant can, respectively, be deduced from (12) as

$$\alpha = -\frac{1}{2l} \times \ln |H(\omega)|, \quad (13)$$

and

$$\beta = -\frac{1}{2l} \times \angle H(\omega). \quad (14)$$

Thus, the attenuation and phase constants are determined using the time domain measurements obtained. The propagation velocity  $v$  (m/s) can be determined using phase constant as

$$v = \frac{\omega}{\beta} = \frac{2\pi f}{\beta}. \quad (15)$$

## 6. Calibration of the measuring system

A TD network analysis technique based on transmission parameters ( $S$ -parameters) to extract frequency-dependent propagation constant is based on taking measurements from both sides of the power cable. However, for long cables, a specific requirement is the restriction of access to only one end of the DUT. This limitation led to the use of TDR and originated from the fact that the DUTs usually have a length of up to several kilometers. Measuring access to both cable ends in that case is not always achievable.

TDR measurements have long been used by many industries for detecting and localizing discontinuities and defects in MV power cables. The calibration method already in use for TDR measurements is taking into account a correction factor which is a number, however, in the presented paper, the correction factor is

frequency-dependent [10, 11]. In this way, the extracted frequency-dependent wave propagation characteristics and consequent cable diagnostic results are more accurate and reliable.

Generally, MV power cables have characteristic impedance in the range of  $25 \Omega$ . As the power cable has an impedance different from that of the MS ( $50 \Omega$ ), a significant reflection occurs at the MS/DUT interface. This reflection is recognized to have a major influence on the precision of the cable response measurement. A calibration procedure has already been developed for such kind of analysis [11]. A physical model of the measuring set-up is made in order to identify and remove the influence of the different effects on the parameters extraction. The MS is modeled as shown in Figure 4 [11].

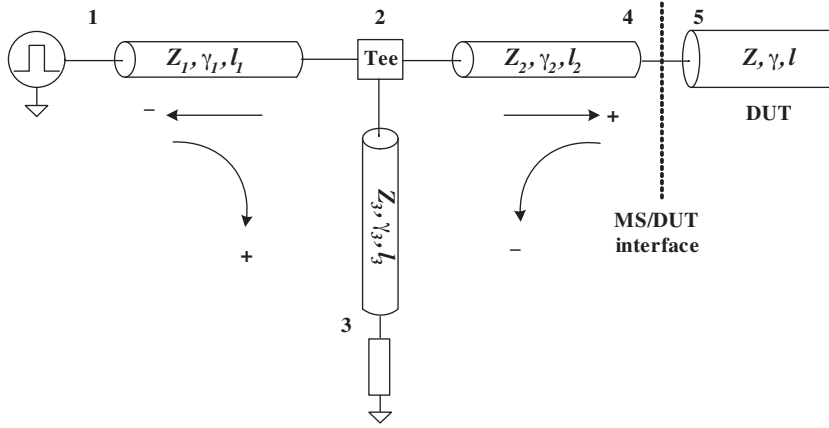


**Figure 4.** Model of the TDR measuring system [9].

In the following equations, the forward and backward traveling waves are indexed with “+” and “-” notation, respectively [7]. The index numbers specify the point at which the voltage is calculated. Points 4 and 5 are at the MS / DUT interface. Point 4 is on the MS side, while point 5 is in the DUT. The measuring point is 3 and all values will be expressed with reference to this point [11].

### 6.1. Forward travelling waves

Assuming that there is perfect match at the “Tee,” the voltage amplitudes at these points are related via the following equations [11]:

$$V_{+2} = V_{+1}e^{-\gamma_1 l_1}, \quad (16)$$

$$V_{+3} = V_{+2}T_t e^{-\gamma_3 l_3}, \quad (17)$$

$$V_{+4} = V_{+2}T_t e^{-\gamma_2 l_2}, \quad (18)$$

$$V_{+5} = V_{+4}T_+ = V_{+4}(1 + \Gamma_+), \quad (19)$$

where  $V_{+1}$  is the voltage amplitude of the source,  $T_t$  is the transmission coefficient of the “Tee” and  $T_+ / \Gamma_+$  is the transmission / reflection coefficient at the MS / DUT interface in the “+” direction.

### 6.2. Backward travelling waves

The following equations hold for backward traveling waves:

$$V_{-4} = V_{-5}T_- = V_{-5}(1 + \Gamma_-) \quad (20)$$

$$V_{-3} = V_{-4}e^{-\gamma_2 l_2} T_t e^{-\gamma_3 l_3}, \quad (21)$$

where  $T_- / \Gamma_-$  is the transmission / reflection coefficient at the MS/DUT interface in the “-” direction. Considering an ideal open-circuit termination, following is valid:

$$e^{-\gamma 2l} = \frac{V_{-5}}{V_{+5}}. \quad (22)$$

Using equations (16)–(21), it can be shown that

$$e^{-\gamma 2l} = \frac{V_{-5}}{V_{+5}} = \frac{V_{-3}}{V_{+3}} \cdot \frac{e^{\gamma_2 2l_2}}{T_t(1 + \Gamma_+)(1 + \Gamma_-)}. \quad (23)$$

It can be concluded from (18) that coaxial lines 1 and 3 have no influence on the extracted propagation constant if we assume a perfect match and the “Tee.” Since  $\Gamma_- = -\Gamma_+$ , the remaining unknowns in (18) are  $\Gamma_+$ ,  $T_t$  and the parameters of the cable 2. The reflection coefficient  $\Gamma_+$  is as

$$\Gamma_+ = \frac{Z - Z_2}{Z + Z_2} = \frac{V_{-4}^m}{V_{+4}}, \quad (24)$$

where the signal  $V_{-4}^m$  reflected at the MS / DUT interface is expressed with reference to measuring point 3 as:

$$V_{-4}^m = \frac{V_{-3}^m}{T_t e^{-\gamma_2 l_2} e^{-\gamma_3 l_3}}. \quad (25)$$

Substitution in (24) using (18), (18), and (15) results in

$$\Gamma_+ = \frac{V_{-3}^m}{V_{+3}} \cdot \frac{1}{T_t e^{-\gamma_2 2l_2}}. \quad (26)$$

If a measurement with the end of coaxial cable 2 short-circuited is considered, it is valid as

$$V_{-3}^{short} = -V_{+1} T_t^2 e^{-\gamma_2 2l_2} e^{-\gamma_3 l_3} \quad (27)$$

and is the measured signal reflected at the short-circuited end of cable 2 and is referred as the incident pulse. Using (16), (17), and (28) and substituting in (23) and (26) by assuming  $Z_1 = Z_2 = Z_3$ , gives as

$$\Gamma_+ = -\frac{V_{-3}^m}{V_{-3}^{short}} \quad (28)$$

$$H(\omega) = e^{-\gamma 2l} = \frac{V_{-3} V_{-3}^{short}}{(V_{-3}^m)^2 - (V_{-3}^{short})^2}, \quad (29)$$

where

$$V_{-3}^{short} = -V_{+3} T_t e^{-\gamma_2 2l_2}. \quad (30)$$

The described extraction technique requires two TDR measurements; one is the DUT response and the other is calibration measurement with cable 2 short-circuited. The incident pulse  $V_{-3}^{short}$ , mismatch reflection  $V_{-3}^m$ , and DUT response  $V_{-3}$  are extracted from these measurements using TD windowing as described in next section. The position of the window frames is chosen at the points where the TDR signal is closest to or equal to zero. The windowed signals are then padded with zeros, so that they have equal lengths, which length is also a multiple of 2. Using FFTs, the pulses are then transferred to the frequency domain, where the frequency-dependent propagation constant and propagation velocity are calculated using (29) and (15), respectively.



## 7. TDR measurements and results

The following two TDR measurements were captured in the data acquisition system then processed in MATLAB for the extraction of wave propagation characteristics from the measurements.

- i. *TDR-DUT response*: This measurement is captured when the DUT is open-circuited. The time domain waveform for this measurement is shown in Figure 5.
- ii. *TDR-calibration*: This measurement is captured when the coaxial cable 2 is short-circuited. The time domain waveform for this measurement is shown in Figure 6.

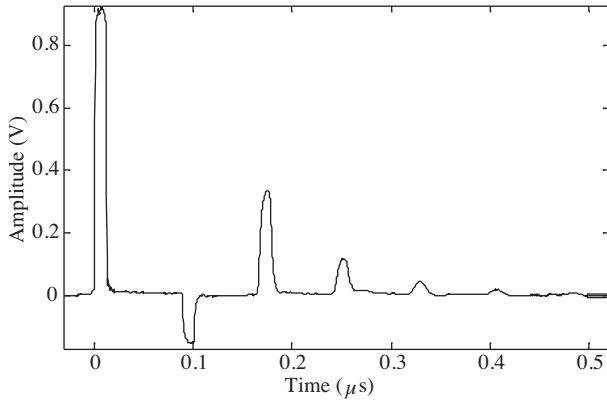


**Figure 5.** TDR response when the DUT is open-circuited.

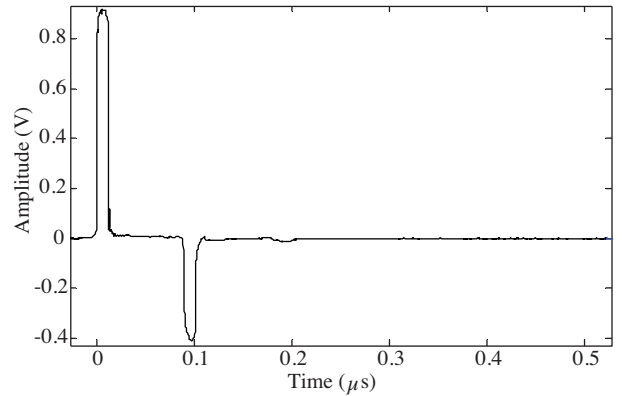


**Figure 6.** TDR response when the coaxial cable 2 is short-circuited.

The mismatch reflection  $V_{-3}^m$  and the DUT response  $V_{-3}$  are extracted from the TDR-DUT response measurement, while the incident pulse  $V_{-3}^{short}$  is extracted from the TDR-calibration measurement. These pulses are taken and padded with zeros up to the length of  $N = 2^n$ , for  $n = 16$ . The modified zero-padded waveforms are shown in Figure 7. The FFTs of the modified zero-padded incident pulse and DUT response are shown in Figure 8. Using FFTs of the modified zero-padded pulses in (29) and (15), the measured attenuation constant and wave propagation velocity in the DUT can be determined, and the dependency of these parameters on the frequency of the propagated signals is shown in Figure 9. A time step of 0.2 ns is used in the Fourier analysis.

## 8. Discussion

The attenuation and propagation velocity of the signal in the cable under investigation are fairly constant at lower frequencies (0.02 dB/m and 154 m/ $\mu$ s), however, these values are frequency-dependent at higher frequencies. In frequency bandwidth beyond 10 MHz, the value of these parameters begins to increase with an increase in frequency of the propagated signals. The significant signal attenuation is attributed to the highly dispersive materials of the conductor insulation/shields and concentric neutral beds. The latter is used for improved potential distribution and mechanical properties at the interface between concentric neutral and the insulation shield.

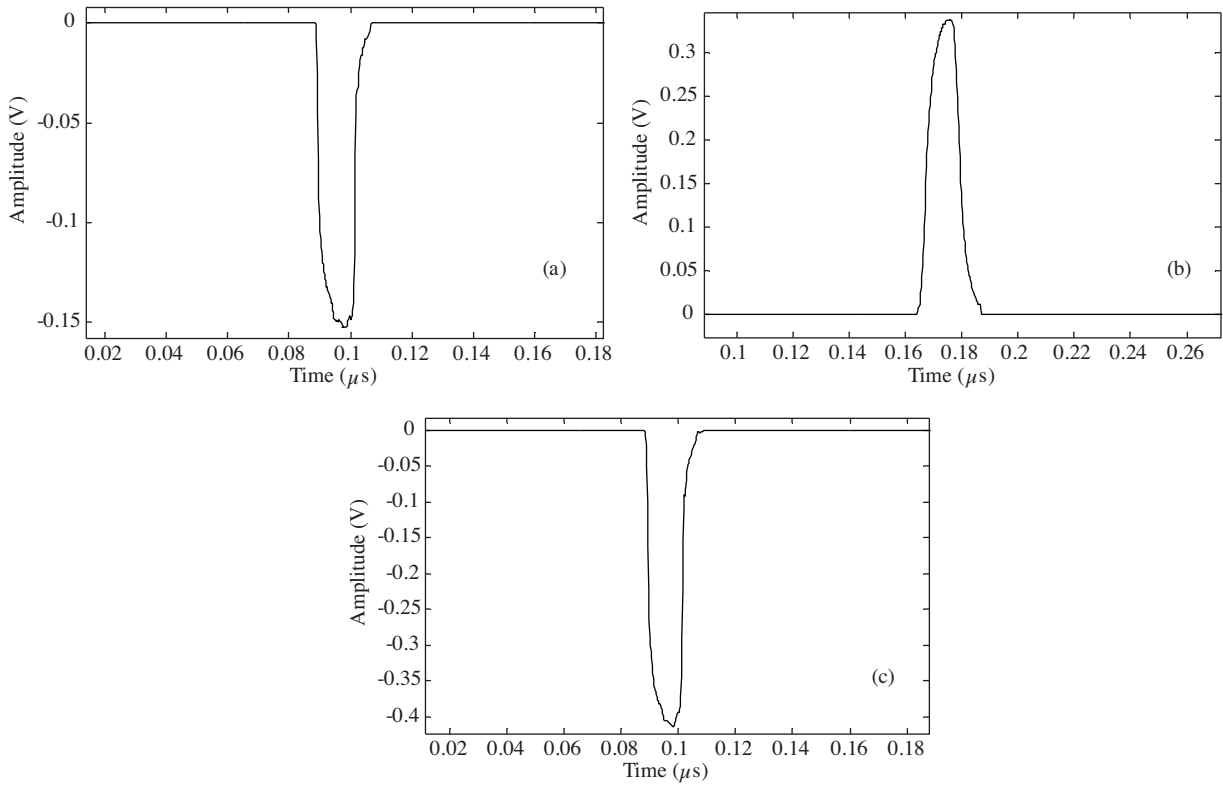


**Figure 7.** Modified zero-padded waveforms: (a) mismatch reflection, (b) DUT response, and (c) incident pulse.

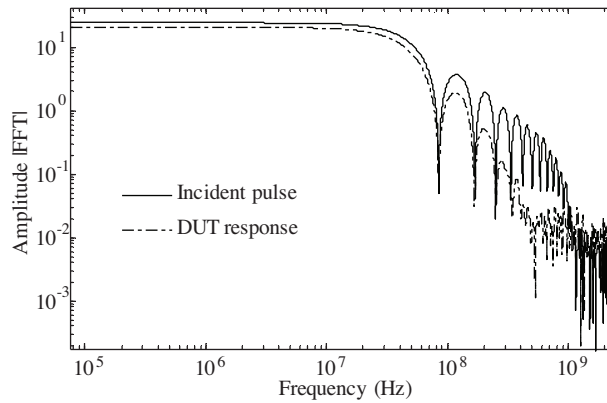


**Figure 8.** FFTs of the incident pulse and the DUT response.

Resolution of the measured wave propagation is good to 81 MHz, beyond which it is lost in the certain repetitive disturbances or noise level. One possible way to explain the disturbances in the measurements is to have a look at the FFTs of the incident pulse and DUT response (see Figure 8). The magnitude of these FFTs remains constant up to 10 MHz, therefore, the attenuation is also constant up to this range of frequency. Beyond this frequency, FFT of the DUT response starts to decrease at a higher rate, resulting in linear increase in the attenuation. Beyond 81 MHz, FFTs suffer in noise and give values different from the actual functions. The noise level has some peaks, which are taken into account instead the actual functions, resulting in the noisy peaks in the attenuation.

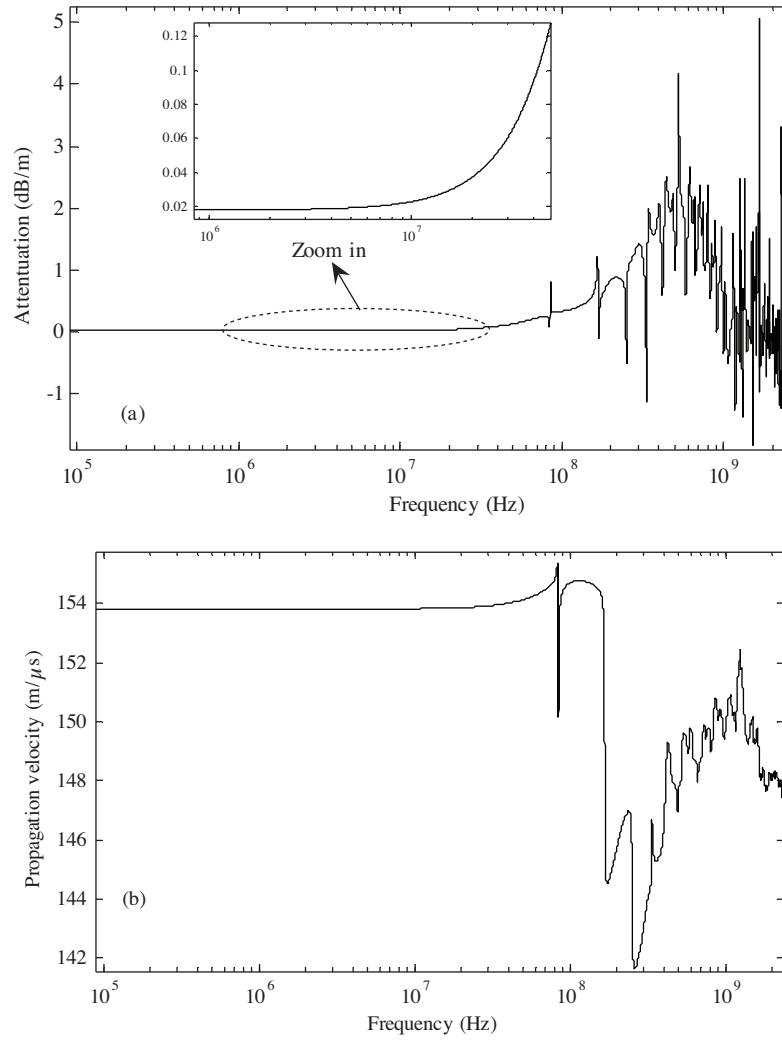


**Figure 9.** Measured wave propagation characteristics of single-phase MV XLPE power cable: (a) attenuation constant, (b) and propagation velocity.

Another mathematical interpretation is on the basis of the Fourier transform function. For an ideal square pulse such as [12]

$$f(t) = \begin{cases} 1, & |t| < a \\ 0, & |t| > a, \end{cases} \quad (31)$$

the analytical Fourier transform function is in the form

$$F[f(t)] = \frac{2 \sin a\omega}{\omega}, \quad \omega > 0. \quad (32)$$

It can be concluded that Fourier transform function would periodically equal to zero. The zero crossings can be defined as

$$f_0 = \frac{k}{2a}, \quad (33)$$

where  $k=1,2,\dots,N$  and  $f_0$  is the frequency at which the Fourier function equals to zero.

In the presented case the pulse width for the incident signal is  $2a = 12$  ns (see Figure 5), so it could be expected that zero crossings and the respective numerical artefacts to be in the vicinity of  $f_0 = 81$  MHz (for  $k = 1$ ).

In this paper, the technique applied to extract frequency-dependent wave propagation characteristics has already been used in [11]. The TDR measurements given in [11] are taken in High Voltage Laboratory, which is free from external interferences. However, TDR measurements given in the presented paper have been taken in an ordinary place to simulate the situation with on-site measurements. A major bottleneck encountered with on-site TDR measurements is the ingress of external interferences that directly affects the sensitivity and reliability of acquired data. The noise sources can be discrete spectral interference (caused by radio broadcasts and communication networks), periodical pulse shaped disturbances (caused by corona discharges, other discharges due to transformers, or power electronics), stochastic pulse shaped disturbances (caused by lightning or switching operations), or white noise (caused by measuring instrument itself) or combination of any of these noises. The given frequency-dependent attenuation and propagation velocity curves suffer from noise at higher frequencies, while this is not the case for these curves given in [11]. The magnitude of attenuation and propagation velocity at different frequencies given in this paper have bit higher values as compared to the values of these parameters given in [11], however, the difference is small which can be neglected. It confirms that the described TDR measuring technique is not only valid for interference free environment, but can also be used in noisy and harsh environment for getting accurate and reliable diagnostic results.

## 9. Conclusions

The TDR measurement technique has been presented to extract the frequency-dependent wave propagation characteristics of single-phase MV XLPE power cables in an ordinary environment. The calibration of the system corrects for the impedance mismatch at the MS/DUT interface by calculating the frequency-dependent reflection coefficient at this point. The calibration additionally removes the symmetric errors from losses in the connecting cables of the MS, thus assuring TDR measurement is more accurate and reliable.

It is revealed that the signal attenuation and propagation velocity in power cable are fairly constant at lower frequencies, but these parameters are frequency-dependent at higher frequencies beyond 10 MHz, i.e., their values increase by increasing the frequency of the propagated signals. The wave propagation characteristics of power cable are changing at different voltage levels because of the difference in cable construction based on insulation design. The TDR measurement results on XLPE power cable can be used to localize the discontinuities as well as the design of communication through distribution power cables.

## References

- [1] G. Mugala, "High Frequency Characteristics of Medium Voltage XLPE Power Cables," *Doctoral Thesis, The Royal Institute of Technology, (KTH)*, Stockholm, Sweden, December 2005.
- [2] R. Papazyan, "Techniques for Localization of Insulation Degradation along Medium-Voltage Power Cables," *Doctoral Thesis, The Royal Institute of Technology, (KTH)*, Stockholm, Sweden, ISBN 91-7178-044-0, April 2005.
- [3] Froroth, "Home Access Communications – Panning out of the Alternatives," Vattenfall and the Royal Institute of Technology (KTH), Stockholm, Sweden. *Proceedings of the Telecom Power Europe, Conference*, London (UK), October 27–28, 1998.

- [4] G. Mugala, R. Papazyan, P. Nakov, "High Frequency Characterization of Medium Voltage Cables using Time Domain Reflectometry Techniques," *Proceedings of 17<sup>th</sup> Nordic Insulation Symposium on Electrical Insulation, NORD-IS'01*, Stockholm, Sweden. pp. 211–218, June 11-13, 2001.
- [5] G. Mugala, R. Eriksson, "High Frequency Characteristics of a Shielded Medium Voltage XLPE Cable," *Proceedings of Conference on Electrical Insulation and Dielectric phenomena, CEIDP'2001*, pp. 132–136, October 2001.
- [6] G. C. Stone, S.A. Boggs, "Propagation of Partial Discharge Pulses in Shielded Power Cables," *Proceedings of Conference on Electrical Insulation and Dielectric phenomena, CEIDP'82*, pp.275–280, October 1982.
- [7] D. K. Cheng, *Field and Wave Electromagnetics*, 2<sup>nd</sup> edition, Addison Wesley Publishing Company, Inc., 1989, pp. 449–471.
- [8] H. Meng, S. Chen, Y. L. Guan, C. L. Law, P. L. So, E. Gunawan, T. T. Lie, "A Transmission Line Model for High-Frequency Power Line Communication Channel," *Proceedings of International Conference on Power System Technology (PowerCon 2002)*, Kunming, China, October 13-17, 2002, pp. 1290–1295.
- [9] R. Papazyan, "Study on Localisation of Water Degraded Regions along Power Cable Insulation using Time Domain Reflectometry," *The Royal Institute of Technology*, Master thesis No. 23030/3 2000.
- [10] G. M. Hashmi "Determination of Propagation Constants of Three Phase MV Cables using Time Domain Reflectometry," *Masters Thesis Work, The Royal Institute of Technology, (KTH)*, Stockholm, Sweden, Feb. 2001.
- [11] R. Papazyan, R. Eriksson, "Calibration for Time Domain Propagation Constant Measurements on Power Cables," *IEEE Transaction on Instrumentation and Measurement*, Vol. 52, No. 2, pp. 415–418, April 2003.
- [12] L. Råde, B. Westergren, *Mathematics Handbook for Science and Engineering*, 3<sup>rd</sup> edition, Chartwell-Bratt, 1995, pp. 312.